RESEARCH ARTICLE
doi: 10.2306/scienceasia1513-1874.2022.134

ScienceAsia 49 (2023): **70–76**

H_2O_2 suppresses ROS elimination and osteogenesis by inhibiting MT2 expression

Qionghua Yao[a], **Jiafu Lin**[a], **Shengwang Wei**[b,*]

[a] Department of Medical College, Fujian Health College, Fuzhou 350101, Fujian China
[b] Department of Orthopaedics, Liuzhou Workers Hospital, Liuzhou 545005, Guangxi China

*Corresponding author, e-mail: wswworkers@163.com

Received 2 Sep 2021, Accepted 4 Jun 2022
Available online 10 Oct 2022

ABSTRACT: Hydrogen peroxide (H_2O_2) can damage the activity of osteoblasts, thus inhibiting the osteogenesis. Metallothionein (MT) is a scavenger of reactive oxygen species (ROS), which can promote the osteogenesis. Our transcriptomic results showed that H_2O_2 decreased the mRNA expression of MT2 in osteoblasts. This study aims to explore the regulatory effect of MT2 gene on the osteogenesis under oxidative stress. In this study, we explored the effect of MT2 on ROS production in osteoblasts by using gene overexpression or silencing. Then, the role of H_2O_2 on MT2 expression in osteoblasts was further observed. Ultimately, the effect of MT2 overexpression on osteogenic capacity under H_2O_2 treatment was investigated. Our results showed that MT2 overexpression reduced ROS production in osteoblasts, while MT2 silencing was contrary. Moreover, MT2 levels in osteoblasts decreased under H_2O_2 intervention. Importantly, MT2 overexpression reversed H_2O_2-inhibited osteoblastic number and activity. In conclusion, this study indicated that H_2O_2 can inhibit ROS scavenging by downregulating MT2 expression, whereby inhibiting the osteogenesis.

KEYWORDS: MT2, H_2O_2, osteogenesis, osteoblast, ROS

INTRODUCTION

Osteoclast-mediated bone resorption and osteoblast-mediated osteogenesis maintain bone homeostasis. The increase of osteoclastic activity or the decrease of the osteoblastic activity could destroy the above balance and lead to osteoporosis. The continuous production of reactive oxygen species (ROS) can cause serious oxidative damage to osteoblast formation, which is one of the main pathologies of osteoporosis [1–3]. Hydrogen peroxide (H_2O_2), the representative type of ROS, can lead to the strong oxidative stress, whereby resulting in protein damage and DNA breaks [4], which eventually causes the reduced osteogenesis [5–8].

Metallothionein (MT) is a low molecular protein in human body, which is widely involved in the regulation of a variety of cellular pathophysiological processes. Previous study showed that MT, a free radical scavenger, could effectively remove the accumulation of free radicals caused by various reasons, which plays a key role in maintaining the redox balance of the body [9, 10]. In addition, MT could protect the oxidative damage from ROS [11]. Previous studies showed that MT could resist oxidative damage caused by ionizing radiation, hyperglycemia, and peroxynitrite [12–14]. Our previous transcriptomic results showed that treatment of H_2O_2 could reduce the expression of MT subtype, MT2, in mouse primary osteoblasts. Accordingly, we speculated that H_2O_2 may inhibit the osteogenesis by inhibiting the expression of MT2. In the current study, combined with the overexpression or silencing of MT2 gene, we used H_2O_2 to treat mouse primary osteoblasts to detect the role of MT2 in the osteoblast formation and survival regulated by H_2O_2.

MATERIALS AND METHODS

Cell isolation and culture

Primary osteoblasts were prepared from the calvaria of newborn mice [15]. In short, the skulls of mice (24 h after birth) were dissected, washed with PBS, and digested in fresh 0.1 mg/ml collagenase type II in alpha-minimal essential Eagle's medium (α-MEM) at 37 °C for 20 min (repeated 5 times). After digestion, the supernatant was mixed and centrifuged to obtain cell pellets. The cells were then maintained in α-MEM containing 10% fetal bovine serum (FBS), 100 U/ml penicillin, and 100 mg/ml streptomycin sulfate, at 37 °C with 5% CO_2. Next, the medium was replaced with α-MEM containing 1% bovine serum albumin (BSA), and the cells were cultured for 16 h before preparing for subsequent experiments. Animal study was approved by the Animal Care and Use Committee of Fujian Health College.

Alkaline phosphatase (ALP) staining and ALP activity analyses

Osteoblasts were evaluated using the corresponding ALP staining kit in accordance with manufacturer's protocols (Beyotime, China). ALP activity was measured using a commercial kit in accordance with manufacturer's protocols (Nanjing Jiancheng Bioengineering Institute, China).

RNA sequencing

After treatment with 100 μM H_2O_2 for 4 days, total RNA was prepared from approximately 5 million H_2O_2-treated cells versus control cells by using TRIzol Reagent (Ambion, USA) in accordance with manufacturer's protocols. Total RNA (2 μg) was subsequently used to prepare RNA-seq library by using NEBNext UltraTM RNA Library Prep Kit for Illumina (NEB, USA), following the manufacturer's protocol. The library preparations were sequenced on an Illumina Hiseq 4000 platform, and paired-end 150 bp reads were generated. Raw data (raw reads) of FASTQ format were processed through in-house Perl scripts. Reads were aligned to release GRCh38 of the mouse genome using TopHat 2 (v2.1.0). Gene expression levels (FPKM, fragments per kilobase of exon model per million mapped reads) were calculated with HTSeq (v 0.5.4 p3). All downstream statistical analyses, including PCA, were performed with edgeR program package.

Quantitative real-time PCR (qRT-PCR) analyses

Total RNA was extracted and purified by Trizol method. cDNA synthesis and quantitative real-time PCR (qRT-PCR) analyses were carried out in accordance with manufacturer's protocols (Takara, Japan). The designed primer sequences are shown in supplementary Table S1.

Western blotting analyses

Total cellular protein was extracted using RIPA buffer (Beyotime, China) and quantified using BCA protein assay kit (Beyotime, China). The proteins were loaded and electrophoresed separately through a 15% SDS-PAGE gel. The separated proteins were subsequently transferred to the polyvinylidene fluoride membranes (PVDF) and incubated with primary antibodies (rabbit anti-MT2, catalase, p47phox, p67phox, and β-actin; Cell Signaling Technology, USA) at 4 °C overnight. After washing, the membrane was incubated with the secondary antibody at room temperature for 60 min. The immunoreactive bands were visualized using an ECL kit (Millipore, USA) and were quantified using a Chemi-Doc image analyzer (Bio-Rad Laboratories, USA).

Lentiviral transduction

Recombinant lentiviruses encoding the wild-type *MT2* or shRNA against *MT2* were constructed by homologous recombination between the expression vector (pEX-Puro-Lv105) and cDNA/shRNA in 293 cells using the lentivirus construction kit in accordance with manufacturer's protocols. The same method was used to construct and package the corresponding control vector. After 2 days, supernatants were harvested, and primary osteoblasts were incubated in medium containing lentiviruses and 5 μg/ml polybrene at the multiplicity of infection (MOI) of 40 for 2 days. The infected cells were selected using puromycin (10 μg/ml). The overexpression efficiency of viral gene was detected using qPCR analysis.

Measurement of intracellular ROS

Treated cells were seeded onto 24-well plates. Next, the intracellular ROS were evaluated using DCFH-DA fluorescent probe (Sigma-Aldrich, USA). Subsequently, the cells were rinsed 3 times with PBS and then incubated with the DCFH-DA fluorescent probe for 25 min. Following rinsing with PBS 3 times, the fluorescence intensity was quantified at 488 nm excitation wavelength and 525 nm emission wavelength using a fluorescent plate reader.

Measurement of NADPH oxidase activity

NADPH oxidase activity was determined by the enhanced lucigenin chemiluminescence method [16]. In short, cells were rinsed 5 times in ice-cold PBS and scraped from the plate in PBS. The cell pellets were centrifuged at 800 g at 4 °C for 10 min and were resuspended in lysis buffer. Cell suspensions were homogenized with 100 strokes in a Dounce homogenizer on ice. Then, 100 μl of homogenate was added into 900 μl of 50 mM phosphate buffer (pH 7.0) containing 1 mM EGTA, 150 mM sucrose, and 5 μM lucigenin as the electron acceptor and 100 μM NADPH as an electron donor. The light emission in terms of relative light units was detected every minute for 10 min with a plate reader spectrophotometer (SpectraMax 190; Molecular Devices, USA). The data representing NADPH oxidase activity were expressed as the mean light units (MLU) per minute per milligram of protein.

Cell proliferation analyses

Cell proliferative levels were detected using cell counting kit-8 in accordance with manufacturer's protocols (Dojindo, China). The optical density at 450 nm (OD450) was measured using Varioskan Flash reader (Thermo Fisher Scientific, USA). Cell proliferation was also evaluated by detecting mRNA expression of proliferating cell nuclear antigen (PCNA).

Cell apoptosis/death analyses

Apoptosis was assessed by detecting Caspase3 activity: Caspase3 activity was measured by ApoAlert caspase fluorescent assay kit (Clontech Laboratories, USA). Treated cells were lysed in 120 μl of lysis buffer and incubated on ice for 10 min. Then, 120 μl of reaction buffer containing 12 μl of 1 mM caspase3 fluorescent substrate were added to each sample and incubated for 1 hour at 37 °C. The fluorescence intensity was quantified using a fluorospectrophotometer (Synergy2, BioTek, USA; excitation at 400 nm and emission at 505 nm). Total cell death levels were detected by trypan blue staining. Treated cells were

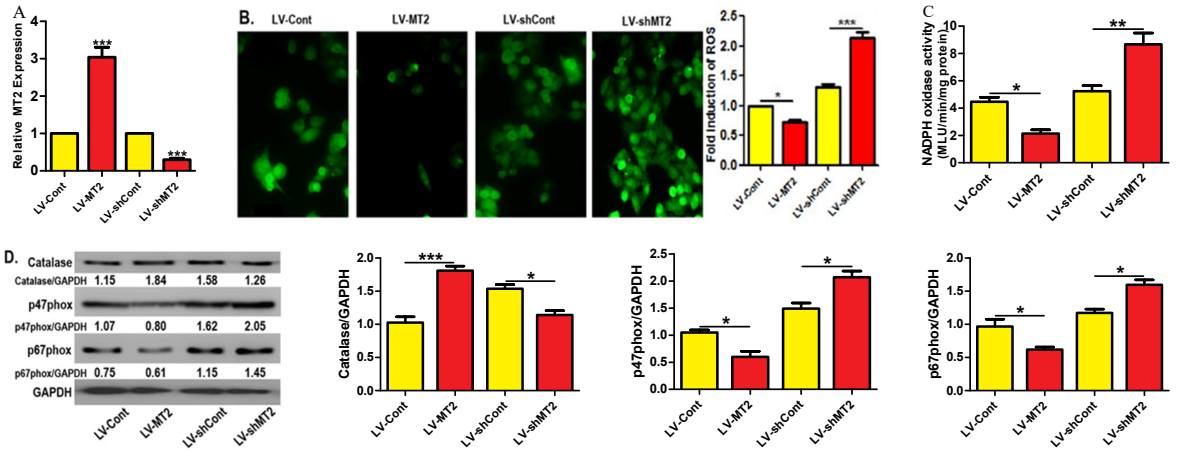

Fig. 1 Relationship between MT2 expression and ROS levels in osteoblasts. (A) mRNA levels of MT2 in osteoblasts infected with lentiviruses encoding MT2-cDNA, MT2-shRNA (LV-MT2, LV-shMT2), and corresponding control vectors. (B) The fluorescence intensity of indicated cells incubated with DCFH-DA fluorescent probe (representative images shown). ROS levels represented as the fold induction by normalizing the fluorescence value of other groups to that of LV-Cont group. (C) NADPH oxidase activity and (D) protein levels of catalase, p47phox, and p67phox in Lentiviruses-transduced cells. Data expressed as mean ± SEM from 3 independent experiments. * $p < 0.05$, *** $p < 0.001$.

suspended, and 0.4% trypan blue solution was added at a volume ratio of 9:1. Subsequently, cells were quantified by an optical microscope. Cells failing to exclude dyes were defined as dead cells. The total death rate = number of dead cells/number of total cells.

Statistical analysis

Data are expressed as mean ± SEM. Statistical analyses were performed using SPSS19.0. For comparison, one-way ANOVA or Student's *t*-test was performed. Tukey test was used for Post-Hoc Multiple Comparisons of one-way ANOVA. Differences were considered significant at a threshold of $p < 0.05$.

RESULTS

MT2 overexpression decreased ROS levels in osteoblasts while MT2 silencing was contrary

We firstly observed the effect of MT2 on ROS production in osteoblasts. To achieve this goal, we used lentiviral transduction technology to overexpress or silence MT2 in mouse primary osteoblasts. As shown in Fig. 1A and B, MT2 overexpression decreased ROS levels in osteoblasts, while MT2 silencing increased ROS levels in osteoblasts. In addition, MT2 overexpression increased catalase expression and decreased p47phox expression, p67phox expression, and NADPH oxidase activity, while MT2 silencing had the opposite effects in osteoblasts (Fig. 1C,D). However, MT2 overexpression had no effects on the proliferation, ALP staining intensity, ALP activity as well as mRNA levels of proliferating cell nuclear antigen (PCNA), Col1, and BGLAP in osteoblasts (Fig. 2A–F). Nevertheless, MT2 silencing reduced all the above osteogenic parameters. Furthermore, MT2 overexpression did not affect caspase3 activity and total death levels in osteoblasts, but MT2 silencing increased the 2 indexes (Fig. 2G,H).

Treatment of H_2O_2 decreased MT2 expression in osteoblasts

Next, we investigated the effect of H_2O_2 on MT2 expression in osteoblasts. First, we performed RNA sequencing between H_2O_2-treated and vehicle (PBS)-treated osteoblasts. Transcriptome analysis revealed a large number of DEGs (Fig. 3A). Compared with the control cells, there were 738 upregulated genes and 479 downregulated genes in H_2O_2-treated osteoblasts (Fig. 3A). Remarkably, it was found that the expression of MT2 was significantly decreased by H_2O_2 administration (Fig. 3B). The RNA sequencing result regarding MT2 was verified by qRT-PCR analyses (Fig. 3C). Besides, it was observed that H_2O_2 at any levels inhibited the proliferative capacity, ALP activity, and mRNA levels of PCNA, Col1, and BGLAP in osteoblasts (Fig. 4A-E). Furthermore, all levels of H_2O_2 enhanced caspase3 activity and total death levels in osteoblasts (Fig. 4F,G). The above results identified the effectiveness of H_2O_2 in this experiment. More importantly, all levels of H_2O_2 reduced MT2 expression in osteoblasts (Fig. 3D), which further confirmed the inhibitory effect of H_2O_2 on MT2 expression.

MT2 overexpression enhanced osteoblast formation and survival in the presence of H_2O_2

We documented that H_2O_2 could suppress MT2 expression and the osteogenic ability in osteoblasts. The role of MT2 in the osteogenic ability regulated by

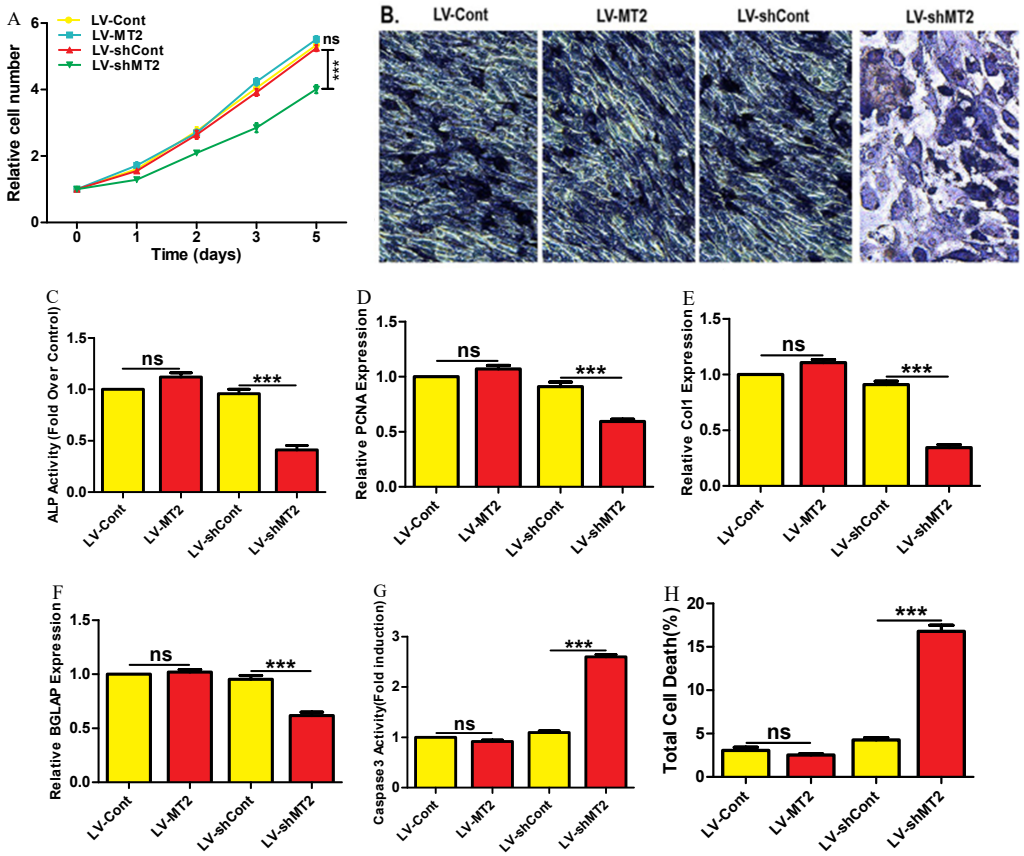

Fig. 2 Role of MT2 silencing in osteoblast formation and survival. (A) The proliferation of treated osteoblasts for indicated time. (B) Osteoblastic differentiation levels of treated cells (LV-Cont, LV-MT2, LV-shCont, and LV-shMT2). (C) ALP activity in osteoblasts following treatment as described in (B). (D–F) mRNA levels of PCNA, Col1, and BGLAP in osteoblasts following treatment as described in (B). (G) The apoptotic levels of osteoblasts following treatment as described in (B) for 4 days. Caspase3 activities represented as the fold induction by normalizing the fluorescence intensity of other groups to that of LV-Cont group. (H) The total death levels of osteoblasts following treatment as described in (B) for 4 days. Data expressed as mean ± SEM from 3 independent experiments. ns, not significant. *** $P < 0.001$.

H_2O_2 required the further investigation. As shown in Fig. 5A, MT2 overexpression decreased ROS levels in osteoblasts under H_2O_2 intervention. In addition, MT2 overexpression reduced the proliferative capacity, ALP activity, and mRNA levels of PCNA, Col1, and BGLAP in osteoblasts under H_2O_2 intervention (Fig. 5B-F). Moreover, both caspase3 activity and total death levels of osteoblasts were also inhibited by MT2 overexpression in the presence of H_2O_2 (Fig. 5G,H).

DISCUSSION

As a typical type of ROS, H_2O_2 strongly threatens the formation of osteoblasts [5–8]. Therefore, it is of great scientific significance to reveal the potential molecular mechanism regarding H_2O_2-inhibited osteogenesis, which is an important challenge in improving the prevention and treatment of osteoporosis. Our team found that MT2 was downregulated in osteoblasts during H_2O_2-treated osteogenesis. Therefore, we hypothesized that MT2, a downstream molecule, alters in expression under H_2O_2 intervention, whereby mediating H_2O_2-inhibited osteogenesis. MT can prevent cells from oxidative damage because of its free radical scavenger property [9, 11]. Here, we also demonstrated for the first time that MT2 protects osteoblast formation and survival from the repression of H_2O_2 due to its inhibitory effect on ROS production.

The inhibitory effect of H_2O_2 on MT2 expression by transcriptomics was confirmed by the detection of mRNA and protein levels *in vitro*. MT2 overexpression significantly reduced ROS levels in osteoblasts with or without H_2O_2. By contrast, MT2 knockdown significantly elevated ROS levels of osteoblasts. The eliminating effect of MT2 on ROS in osteoblasts was identified. It should be noted that in the absence of H_2O_2, MT2 also showed the scavenging effect on basic ROS. Our experimental data showed that MT2 could promote catalase expression and inhibit the expression

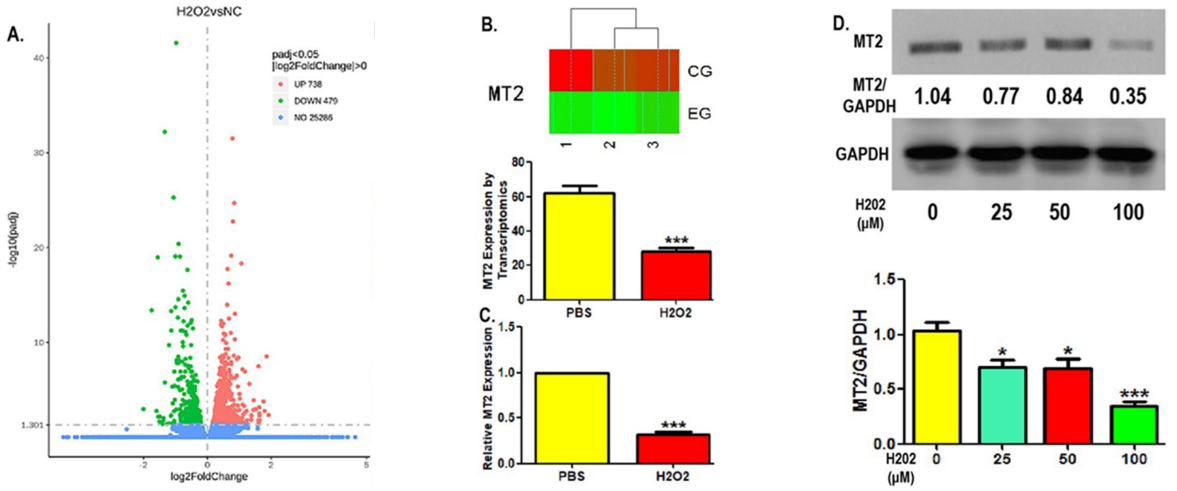

Fig. 3 Role of H_2O_2 in MT2 expression of osteoblasts. (A) Volcano plot representing differential expression analysis of genes regarding RNA sequencing between H_2O_2-treated and control osteoblasts ($n = 3$, each group). The X-axis showing $\log_2$ Fold change in expression; the negative $\log_{10}$ of the p-value plotted on the Y-axis. Each gene represented by one point on the graph. (B) Heat map representing the differential expression analysis of MT2 between H_2O_2-treated and control osteoblasts ($n = 3$, each group). (C) mRNA levels of MT2 in H_2O_2-treated and control osteoblasts and (D) MT2 protein levels following treatment with 100 μm H_2O_2 for 4 days. Data expressed as mean ± SEM from 3 independent experiments. * $P < 0.05$, *** $P < 0.001$. NC/CG, control osteoblasts treated with PBS; EG, H_2O_2-treated osteoblasts.

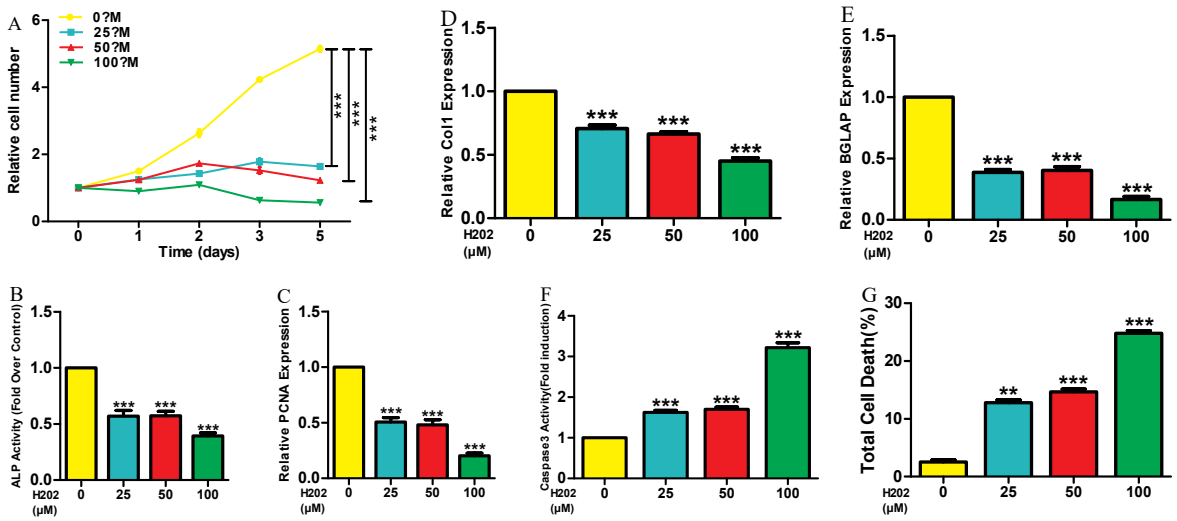

Fig. 4 Role of H2O2 in osteoblast formation and survival. (A) The proliferation of treated osteoblasts following treatment with different concentrations of H_2O_2. (B) ALP activity in osteoblasts following treatment with different levels of H_2O_2 for 7 days. (C–E) mRNA levels of PCNA, Col1, and BGLAP in osteoblasts following treatment with different levels of H_2O_2 for 7 days. (F) The apoptotic levels of osteoblasts following treatment with different levels of H_2O_2 for 4 days. Caspase3 activities represented as the fold induction by normalizing the fluorescence intensity of other groups to that of control group (0 μm H_2O_2). (G) The total death levels of osteoblasts following treatment with different levels of H_2O_2 for 4 days. Data expressed as mean ± SEM from 3 independent experiments. *** $P < 0.001$.

of p47phox and p67phox as well as NADPH oxidase activity. MT is capable of eliminating the accumulation of free radicals caused by multiple reasons, thus maintaining the redox balance of the body [9, 10]. The production of ROS can depend on NADPH oxidase [16]. It was suggested that as a subtype of MT, MT2 can regulate NADPH oxidase activity by changing the expression of corresponding effector molecules, thus altering the accumulation of basic ROS in osteoblasts. In addition, the alteration of catalase levels also indicated

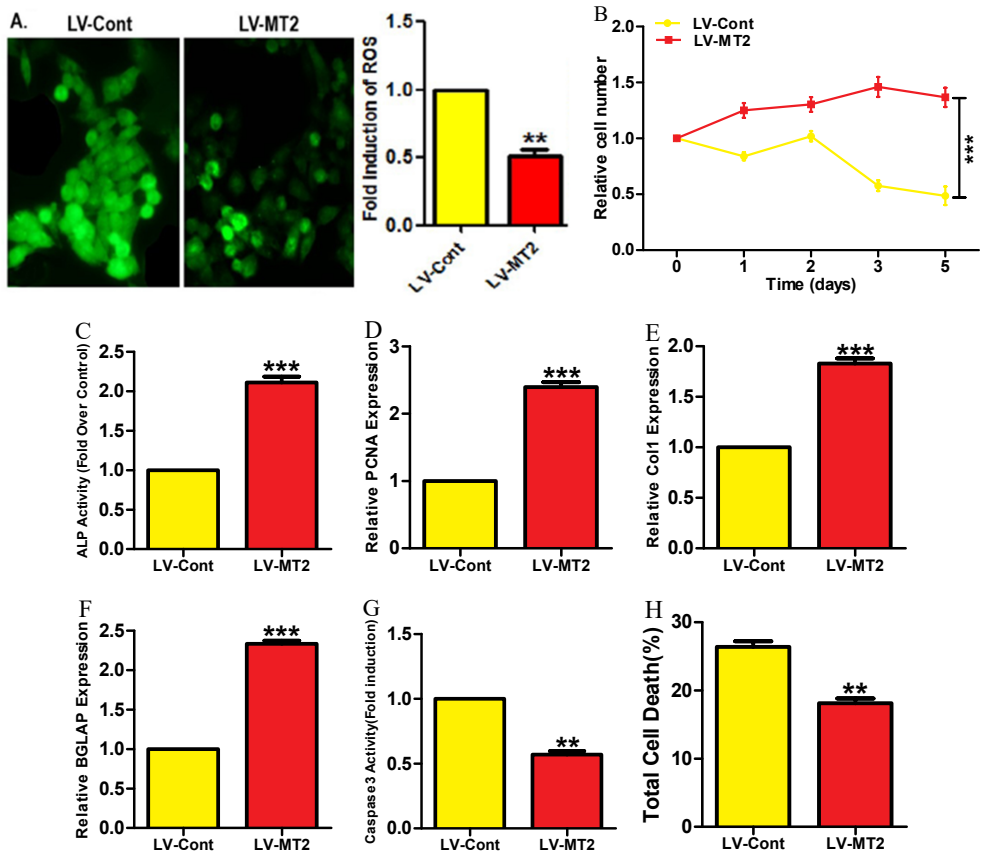

Fig. 5 Role of MT2 in osteoblast formation and survival regulated by H_2O_2. (A) The fluorescence intensity of indicated cells incubated with DCFH-DA fluorescent probe (representative images shown) following treatment with 100 μm H_2O_2 for 2 days. ROS levels represented as the fold induction by normalizing the fluorescence value of LV-MT2 group to that of LV-Cont group. (B) The proliferation of indicated osteoblasts treated with H_2O_2 for different times. (C) ALP activity in indicated osteoblasts treated with H_2O_2 for 7 days. (D–F) mRNA levels of PCNA, Col1, and BGLAP in osteoblasts following treatment as described in (C). (G) The apoptotic levels of indicated osteoblasts following treatment as described in (C) for 4 days. Caspase3 activity represented as the fold induction by normalizing the fluorescence intensity of LV-MT2 group to that of LV-Cont group. (H) The total death levels of osteoblasts following treatment as described in (C) for 4 days. Data expressed as mean ± SEM from 3 independent experiments. ** $P < 0.01$, *** $P < 0.001$.

that in the presence of H_2O_2, MT2 can prevent the oxidative stress caused by H_2O_2 by catalyzing H_2O_2 decomposition. In addition, MT2 knockdown significantly inhibited the osteogenic activity and osteoblast survival. Although MT2 overexpression did not affect the osteogenic activity and osteoblast survival, MT2 overexpression significantly improved the osteogenic activity and osteoblast survival inhibited by H_2O_2. The generation of ROS can bring serious oxidative damage to osteoblasts, thereby causing the reduced osteogenesis [1–8]. The above results support the role of MT2 in promoting the osteogenesis, especially under oxidative stress, which is due to its scavenging effect on ROS. It was noted that MT2 overexpression enhanced osteoblast formation and survival in the presence of H_2O_2, whereas MT2 overexpression did not affect the above parameters under normal conditions. The reason might be that in the absence of H_2O_2, ROS levels in osteoblasts are rather low, resulting in the fact that ROS accumulation is not the main factor affecting the osteogenesis. Therefore, ROS production slightly regulated by MT2 overexpression could not effectively affect osteoblast formation. In addition, the regulatory mechanism of H_2O_2 on MT2 expression needs to be further explored in future.

In conclusion, our experimental results provided the first evidence for the underlying mechanism of osteogenesis under oxidative stress: H_2O_2 can inhibit MT2 expression, thus attenuating the eliminating of ROS, which ultimately suppresses osteoblast formation and survival. The current data shed light on the prevention and treatment of osteoporosis.

Appendix A. Supplementary data

Supplementary data associated with this article can be found at http://dx.doi.org/10.2306/scienceasia1513-1874.2022.134. All data used to support the findings of this study are available from the corresponding author upon reasonable request.

Acknowledgements: This work was supported by Fujian health and family planning youth research project (2016-1-83).

REFERENCES

1. Frenkel B, White W, Tuckermann J (2015) Glucocorticoid induced osteoporosis. *Adv Exp Med Biol* **872**, 179–215.
2. Manolagas SC (2010) From estrogen-centric to aging and oxidative stress: a revised perspective of the pathogenesis of osteoporosis. *Endocr Rev* **31**, 266–300.
3. Schroder K (2019) NADPH oxidases in bone homeostasis and osteoporosis. *Free Radic Biol Med* **132**, 67–72.
4. Lee YM, Kim IS, Lim BO (2021) Effect of sandalwood oil on inhibition of reactive oxygen species generation and lipopolysaccharide-induced inflammation through down-regulation of the nuclear factor-κB signaling pathways. *ScienceAsia* **47**, 277–286.
5. Liang J, Shen YC, Zhang XY, Chen C, Zhao H, Hu J (2020) Circular RNA HIPK3 downregulation mediates hydrogen peroxide-induced cytotoxicity in human osteoblasts. *Aging* **12**, 1159–1170.
6. Ruan JW, Yao C, Bai JY, Zhou XZ (2018) microRNA-29a inhibition induces Gab1 upregulation to protect OB-6 human osteoblasts from hydrogen peroxide. *Biochem Biophys Res Commun* **503**, 607–614.
7. Zheng Y, Chen Z, She C, Lin Y, Hong Y, Shi L, Zhang Y, Cao P, Xu X (2020) Four-octyl itaconate activates Nrf2 cascade to protect osteoblasts from hydrogen peroxide-induced oxidative injury. *Cell Death Dis* **11**, 772.
8. Zhu X, Zhao Z, Zeng C, Chen B, Huang H, Chen Y, Zhou Q, Yang L, et al (2020) HNGF6A inhibits oxidative stress-induced MC3T3-E1 cell apoptosis and osteoblast phenotype inhibition by targeting Circ_0001843/miR-214 pathway. *Calcif Tissue Int* **106**, 518–532.
9. Kovalchuk O, Burke P, Besplug J, Slovack M, Filkowski J, Pogribny I (2004) Methylation changes in muscle and liver tissues of male and female mice exposed to acute and chronic low-dose X-ray-irradiation. *Murat Res* **548**, 75–84.
10. Xue T, Li X, Zhu W, Wu C, Yang G, Zheng C (2009) Cotton metallothionein GhMT3a, a reactive oxygen species scavenger, increased tolerance against abiotic stress in transgenic tobacco and yeast. *J Exp Bot* **60**, 339–349.
11. Kang YJ (1999) The antioxidant function of metallothionein in the heart. *Proc Soc Exp Biol Med* **222**, 263–273.
12. Cai L, Klein JB, Kang YJ (2000) Metallothionein inhibits peroxynitrite-induced DNA and lipoprotein damage. *J Biol Chem* **275**, 38957–38960.
13. Cai L, Cherian MG (2003) Zinc-metallothionein protects from DNA damage induced by radiation better than glutathione and copper- or cadmium-metallothioneins. *Toxicol Lett* **136**, 193–198.
14. Liang Q, Carlson EC, Donthi RV, Kralik PM, Shen X, Epstein PN (2002) Overexpression of metallothionein reduces diabetic cardiomyopathy. *Diabetes* **51**, 174–181.
15. Huang B, Wang W, Li Q, Wang Z, Yan B, Zhang Z, Wang L, Huang M, et al (2016) Osteoblasts secrete Cxcl9 to regulate angiogenesis in bone. *Nat Commun* **7**, 13885.
16. Kang Y, Ding L, Dai H, Wang F, Zhou H, Gao Q, Xiong X, Zhang F, et al (2019) Intermedin in paraventricular nucleus attenuates Ang II-induced sympathoexcitation through the inhibition of NADPH oxidase-dependent ROS generation in obese rats with hypertension. *Int J Mol Sci* **20**, 4217.

Appendix A. Supplementary data

Table S1 Specific primer sequences for qPCR.

Gene	Forward (5′–3′)	Reverse (5′–3′)
MT2	TGCTGACGGGATTTCTGGGAGAG	TAGGCGAGCCACTATCTCAAGGAC
PCNA	GAAGTTTTCTGCAAGTGGAGAG	CAGGCTCATTCATCTCTATGGT
Col1	AGAACAGCGTGGCCT	TCCGGTGTGACTCGT
BGLAP	AGCAGCTTGGCCCAGACCTA	TAGCGCCGGAGTCTGTTCACTAC
GAPDH	ACCACAGTCCATGCCATCAC	TCCACCACCCTGTTGCTGTA